Space Shuttle Orbiter Molecular Environment Induced by the Supplemental Flash Evaporator System

H. K. F. Ehlers*
NASA Johnson Space Center, Houston, Texas

The water vapor environment of the Space Shuttle Orbiter induced by the supplemental flash evaporator during the on-orbit flight phase has been analyzed based on mathematical model predictions and orbital flight measurements. Model data of local density, column density, and return flux are presented to demonstrate the dependence of these data on various parameters, including instrument direction and field of view, as well as Orbiter velocity direction. Results of return flux measurements with a mass spectrometer during STS-2 and of direct flux measurements during STS-4 are discussed and compared with model predictions. Measured and predicted return flux data agree within an order of magnitude. The direct flux data indicate a significantly reduced level of water in the environment above the payload bay when the elevons are in an upward position.

Introduction

ONE of the major contaminants within the Space Shuttle Orbiter environment is water (H_2O). The adverse effects of water on scientific measurements are largely due to strong molecular emission/absorption bands, as well as light scattering by water ice particles. Therefore specific goals for limiting water levels in the Orbiter environment were defined early in the Space Shuttle program.[1,2] Major sources of water are material outgassing, reaction control system (RCS) thrusters, leaks, and dumps. Some results of measurements performed during the STS-2 through STS-4 missions have been previously reported.[3,4]

One significant source of water on orbit is the supplemental flash evaporator system (FES). The purpose of the FES is to augment the Orbiter heat rejection system as well as to serve as an additional water outlet. Mathematical modeling and experimental results are being used to define the environment induced by this system for specific payloads and applications; however, this information is not yet generally available. In this paper, therefore, model predictions are presented in parametric form to provide for a broad understanding of the system's environmental impact. This data base is supplemented by a discussion of some measurement results from early STS missions.

Flash Evaporator Characteristics

The system design was tested and the evaporator flow distribution carefully measured in the early part of the program.[5,6] As a result, the local flux F (g/cm^2-s) from one vent (except in the immediate vicinity of the vent) can be described by

$$F(r,\theta) = (A/r^2)\cos^6(0.608\theta), \quad 0\ \text{deg} \le \theta \le 148\ \text{deg} \qquad (1)$$

where θ (deg) is the angle between the vent centerline and the flow direction, r (cm) is the distance from the vent exit plane, and A (g/s) is a factor which depends on the total flow rate. The flow rate is controlled by a solenoid pulser valve, which is operated with a fixed "on-time" of 200 ms and an on-off pulsing frequency variable between 0 and 4 Hz and thus allows the duty cycle to be varied. Once activated, FES startup and shutoff are programmed to maintain the Freon loop cooling system outlet temperature within a band of 39 ± 1°F, and the flow rate depends on the heat rejection rate.

No significant quantity of ice particles was detected during the system's test. This result justifies the use of Eq. (1) for the total amount of H_2O emitted.

The locations of the FES vents on the Orbiter are the result of operational considerations and tradeoff studies of environmental effects using mathematical modeling. The two vents are placed symmetrically on each side of the fuselage at locations $X = 1506$ in., $Y = \pm 127$ in., and $Z = 305$ in. in the Orbiter coordinate system, as shown in Fig. 1. This information, together with the flow rate, forms the source characteristics input to the mathematical model. Actual flow rates were used for the evaluation of measured flight data. The predicted parametric data presented in the next section are based on a maximum flow rate of 4.4 g/s per vent, for which $A = 1.963$ g/s.

Theoretical Background

The predicted data discussed here are based on the Shuttle/payload contamination evaluation (Space II) model,[7] which describes the molecular environment in terms of parameters such as local density, column density, direct flux, and return flux (including deposition). The predictions depend on Orbiter configuration, contamination source characteristics, Orbiter trajectory/attitude, ambient environment, instrument field of view, etc. Predicted direct fluxes involving "points in space," as well as surfaces, are based on line-of-sight (LOS) view factor, distance, and direction calculation techniques. Density and column density are derived from direct flux predictions. One surface reflection (no deposition) was permitted to derive the predicted data in this paper. Collisions of H_2O molecules with ambient atmospheric molecules will influence the H_2O density distribution to some extent, depending on Orbiter attitude, altitude, etc.; however, they have not been considered here. Calculation of the backscattering return flux of contamination molecules leaving the Space Shuttle Orbiter is founded on the Bhatnagar-Gross-Krook[8] model of collision processes in a binary mixture of gases. This model is an approximation of the Boltzmann kinetic equation. The Space II program implements a solution developed by Robertson.[9]

The following section provides an overview of the characteristics of that part of the Orbiter molecular environment which is induced by an operating supplemental FES. Predictions are presented in parametric form. Some variables such as the ambient density or the prime measurement point (PMP) location are kept constant.

Although a medium total ambient density of 3×10^9 molecules/cm^3 is assumed (corresponding approximately to a medium density at an altitude of 240 km), the return flux predictions may be reasonably extrapolated to other density

Presented as Paper 85-0951 at the AIAA 20th Thermophysics Conference, Williamsburg, VA, June 19-21, 1985; revision submitted Dec. 20, 1985.

*Physicist.

values for higher altitudes. The PMP defines the origin of the LOSs and the receiver locations for return flux. It is assumed to be at Orbiter location $X_0 = 1107$ in., $Y_0 = 0$ in., and $Z_0 = 507$ in. in the Orbiter coordinate system (see Fig. 1). This system has the $+X$ direction pointing aft, the $+Y$ direction to the right of the pilot, and the $+Z$ direction straight out of the (open) payload bay. This PMP location provides for an unobstructed field of view of 2 π sr in the $+Z$ direction, except for a very narrow range occupied by the vertical stabilizer (tail). Shadowing by the tail in the XZ plane occurs for directions with an angle to the $+Z$ direction larger than approximately 57½ deg. For measurement points located closer to the bottom of the bay, the field of view will be smaller, limited by the boundaries of the bay, the orbital maneuvering system (OMS) pods, the tail, other payloads, the remote manipulator system (RMS), etc. These considerations are also valid for return flux. Water from the FES can reach the area above the payload bay mainly via reflection off the elevons and wings. Elevons reflect about six times more than do wings. Reflection rates depend on angle of reflection and therefore vary with elevon position. In an elevon-down position, for instance, the FES exhaust will be reflected more aft, in the $+X$ direction, as compared with the case of zero elevon position. The direct flow from the vents is largely sideways. We begin with the discussion of predictions related to zero position of the elevons as shown in Fig. 1 and will discuss the case for an elevon-up position later.

Local Density

Figure 2 shows typical curves of density vs distance for LOSs in the $+Z/-Y$ quadrant (marked by $\phi = 270$ deg); θ is the angle between the LOS and the $+Z$ axis, and ϕ is the angle with the $+X$ axis in the XY plane measured counterclockwise. The distance r is measured from the PMP. For extrapolation beyond 100 m, a $1/r^2$ dependence may be assumed. The density in grams per cubic centimeter may be converted into units of molecules per cubic centimeter by multiplying by a factor of 3.3×10^{22}. Generally, the density first increases with distance and then, after reaching a maximum, decreases. Close to the PMP the density is low, since the payload bay does not contain major H_2O sources. With increasing θ, the LOS points more to the direction of the vent axis and therefore toward higher densities.

An isodensity surface (surface of constant density) in Fig. 3 shows higher concentration aft of the PMP as well as aft of the vents, a result of the reflections off the wing. As expected, the density is higher in the directions of the vent axes and lower in the XZ plane, which lacks direct flow from the vents.

Column Density

The column density (CD) is the density integrated over a line of sight. It varies with the LOS direction as demonstrated in Fig. 4. Figure 4a shows the CD values in the ZY plane. The lowest value appears in the Z direction receiving no direct source flow; maximum values are calculated in the $\pm Y$ directions corresponding to the direction of the vent axes. The predictions for directions in the ZX plane are seen in Fig. 4b.

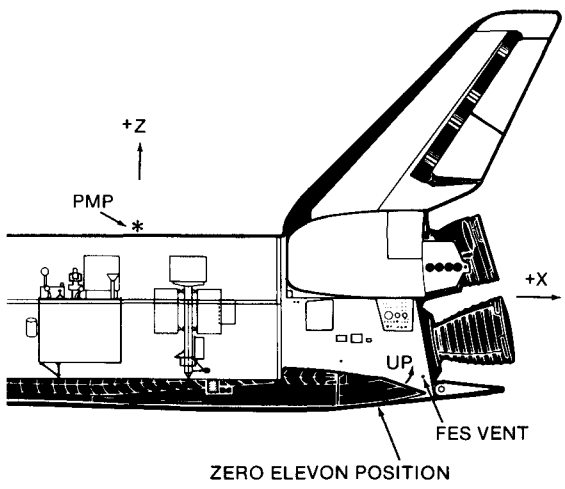

Fig. 1 Geometry for math modeling.

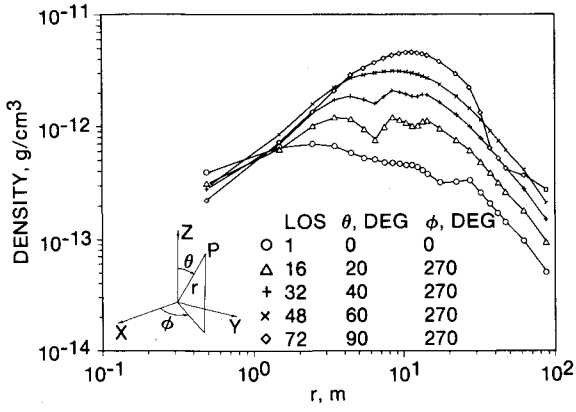

Fig. 2 Water density along some lines of sight in the $+Z/-Y$ quadrant: θ = angle with the $+Z$ axis and ϕ = angle with the $+X$ axis.

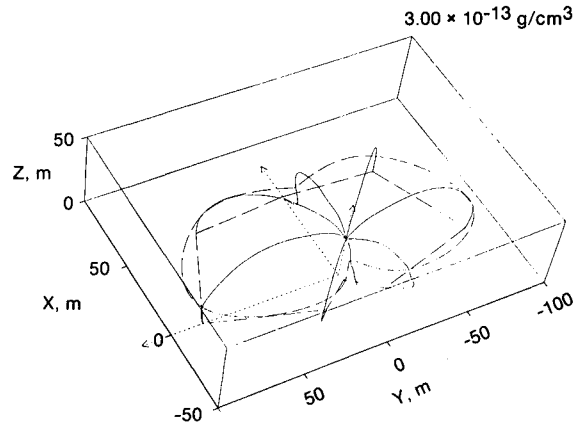

Fig. 3 The H_2O isodensity surface. The Orbiter prime measurement point is at location (0,0,0).

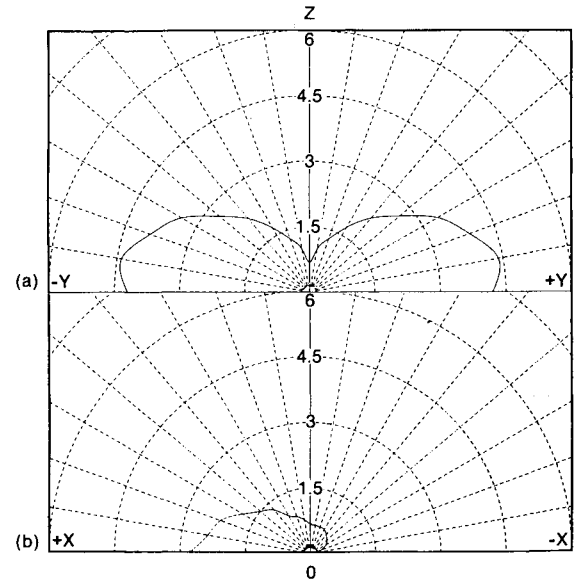

Fig. 4 The H_2O column density, 10^{14} molecules/cm^2, in (a) the ZY plane and (b) the ZX plane.

Here the minimum is in the $-X$ direction (forward), with CDs increasing to a maximum in the $+X$ direction (aft) because of the angle of reflection off the wing/elevon.

Return Flux

The return flux (RF), or backscattering, is the result of collisions of source molecules with ambient or other source molecules. The RF depends on the receiver location/orientation/field of view, the velocity distribution of molecules, contaminant and ambient densities, collision frequency, Orbiter velocity vector, etc. Unless stated otherwise, a field of view of 0.1 sr is assumed. Figure 5 represents the case in which Orbiter velocity is in the $+Z$ direction. In Fig. 5a, the instrument (receiver) axis direction varies in the ZY plane. Minimum RF occurs in the $\pm Y$ direction, which is normal to the velocity vector but in the direction of the vent axes. Interestingly, maximum RF is neither in the $+Z$ nor in the $\pm Y$ direction but, rather, somewhere in between. Figure 5b shows the changes with instrument direction in the ZX plane. Minimum values are found in $\pm X$ directions, whereas the maximum falls between the $+Z$ and $+X$ directions.

The case in which the instrument axis is fixed in the $+Z$ direction while the Orbiter (velocity vector) is rotating is shown in Fig. 6. The results for Orbiter roll are seen in Fig. 6a. When the Orbiter rolls in this case to move in a $+Y$ (or $-Y$) direction, the direction of one vent axis, the measured RF is minimal. Because of its narrow field of view, the instrument simply does not register many of the returning molecules. A somewhat similar situation exists for Orbiter pitch, shown in Fig. 6b.

When the Orbiter moves steadily in a $+Y$ (or $-Y$) direction while the instrument direction varies in the ZY plane, the situation shown in Fig. 7a results. When the instrument rotates to also point into the direction of velocity and one vent axis, a maximum RF is measured in this direction. Similar conclusions can be drawn from the case presented in Fig. 7b. Here the instrument points constantly into a $+Y$ (or $-Y$) direction at various Orbiter roll positions.

The RF plots displayed outline the parametric characteristics when the instrument field of view is constant and relatively narrow (0.1 sr). Obviously, combinations of instrument direction and Orbiter attitude can be found which minimize the RF.

The content of Fig. 8 extends the predictions of RF to instruments with larger fields of view (half-angles). The parameter that yields the family of curves is the angle between the receiver axis, which is parallel to the Orbiter $+Z$ axis, and the Orbiter velocity vector (angle of attack). Figure 8 shows a generally steep increase in RF with an increase in the field of view, except near the 90 deg angle. The decrease of RF with increasing angle of attack is characteristic. Note that there still is significant RF at angles of attack larger than 90 deg and large fields of view. Slowly moving contamination molecules can, after colliding with much faster ambient molecules, still reach a wide-angled receiver in this case. The curve overlap seen in Fig. 8 is due to the 90 deg angle between the main flow and receiver directions.

Elevon-Up Position

For the purposes of this discussion, an elevon-up position is represented by an elevon position above zero that prevents direct H_2O flux from the vents from impinging on the top

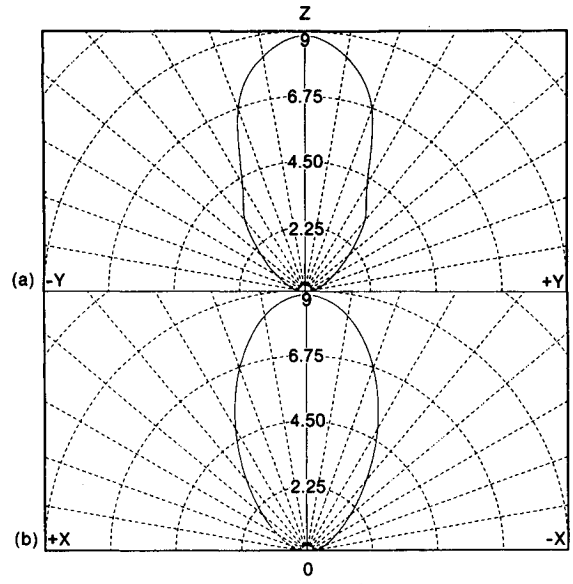

Fig. 6 Return flux, 10^{12} H_2O molecules/cm^2-s-0.1 sr, with receiver in the $+Z$ direction, with Orbiter velocity direction varying in (a) the ZY plane and (b) the ZX plane.

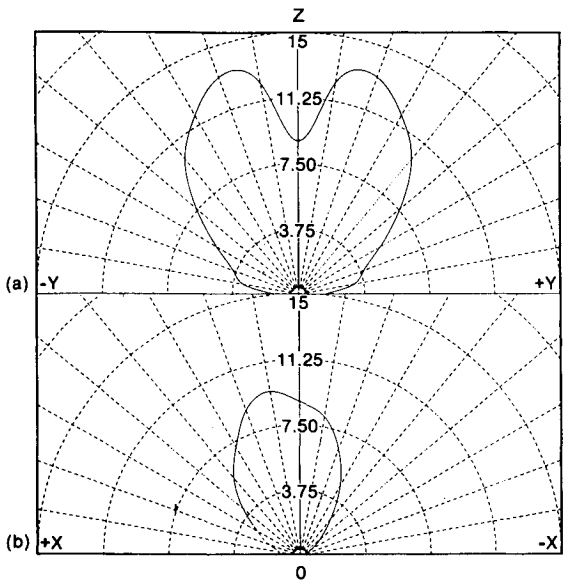

Fig. 5 Return flux, 10^{12} H_2O molecules/cm^2-s-0.1 sr, with receiver direction varying in (a) the ZY plane and (b) the ZX plane (orbiter velocity in the $+Z$ direction).

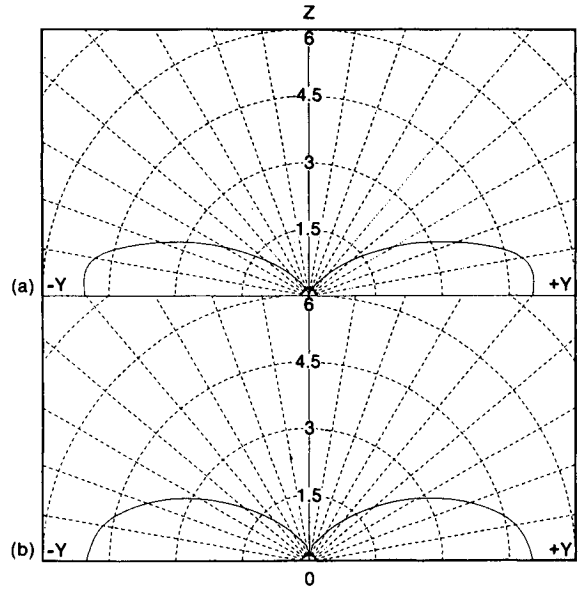

Fig. 7 Return flux, 10^{13} H_2O molecules/cm^2-s-0.1 sr, (a) Orbiter velocity direction: $+Y$(or $-Y$), instrument direction varies, (b) instrument direction: $+Y$(or $-Y$), Orbiter direction varies.

wing/elevon surfaces. Because with the elevon in a zero or lower position the largest contribution of H_2O density above the payload bay comes from direct reflections off the top wing/elevon surfaces, this portion of the density will be eliminated in an elevon-up position. The remaining surfaces exposed to direct flow from the vent are the bottom parts of the OMS pods and the payload bay doors, as well as the sides of the fuselage. Water vapor reflected off these surfaces must be reflected again by the wings to reach the area above the bay. The result is a relatively small contribution. Another small contribution is added by a fraction of flow passing through the gap betwen the elevon and the fuselage along the fuselage to the payload bay region. Calculations of these flows, although theoretically possible, have not been performed to an acceptable level of accuracy because they require special model refinement in areas such as the bottom sides of the OMS pods and doors. In summary, placing the elevons in an upward position appears to be an effective method of significantly reducing H_2O density above the bay during flash evaporator operation. This method of contamination reduction is discussed further in the following section.

Measurements and Results

Neutral, as well as ionized, H_2O molecules in the Orbiter environment were measured with mass spectrometers (MSs) during missions STS-2 through STS-4, whereas particles, including ice, were observed with cameras. Results indicate that the MS of the induced environment contamination monitor (IECM) identified water flow from the FES. The MS is characterized[10] by a mass range of 1-150 amu, a scanning rate of 1 amu/2s, and a field of view defined for many gases, including H_2O, by a gas inlet system containing a zirconium getter pump. The normal cycle time is 10 min, half of which is dedicated to a full spectrum and the other half to amu 18. In a fast mode, however, the MS scans 10 times faster. The MS system, including a collimator, contains several volumes separated by conductances and two zirconium getter pumps; one pump is connected to the collimator and the other to the analyzer section. The collimator allows flux entering the MS from within a cone with a half-angle of about 10 deg to pass through to the ion source without surface contact. Molecules entering from outside this cone are first caught in the collimator; many, but not all, are pulled into its getter pump. This condition necessitates a detailed flow analysis and a development of gas kinetic equations relating ion source density to the directional input flux and to the finite pumping speeds of the collimator and the appendage pumps. These calculations are different for each individual measurement when the incoming flux is not random and are aided by the Space II program.

Two types of measurements were performed: First, RF was measured with the MS in a fixed position pointed toward the Orbiter $+Z$ direction; second, direct flux was measured from the sources during the payload bay survey when the IECM was positioned by the RMS.

RF Measurements

Measurements of H_2O RF from the FES were successful during the Z local vertical attitude (bay to Earth) of the STS-2 mission. Identification and quantification of the FES-related mass peaks were simplified by the constant Orbiter attitude and therefore stationary velocity vector. The MS response for amu 18 between 16 and 33 h mission elapsed time (MET) is shown in Fig. 9. The period from 16 to 21 h MET is an inactive portion of the mission, without FES operation, marked by variation of MS output with the day/night cycle. The 5-min intervals of amu 18 output are clearly discernible. During the following period, between 22 and 33 h MET, the FES operated intermittently, mainly during daytime, as indicated by the letters (b)-(d) and (f)-(h) in Fig. 9. The FES flow rate varies with the heat load rejected and decreases to zero below the Freon loop coolant temperature of 39°F. This cutoff temperature

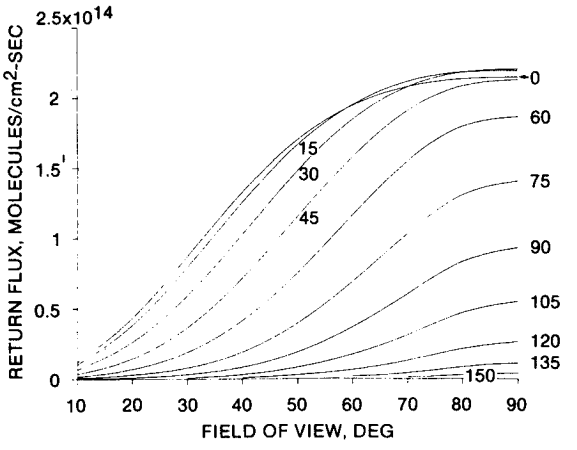

Fig. 8 The H_2O return flux as a function of receiver field of view for various angles (deg) between the Orbiter velocity vector and the Orbiter $+Z$ axis within the $+Z/-Y$ quadrant.

limit was reached during nighttime. Note that the character of the peaks changed markedly at about 27.5 h MET following a maneuver resulting from a series of RMS/RCS tests. As compared with peaks (b)-(d), the peaks (f)-(h) have a higher amplitude, with numerous superimposed high, narrow peaks indicating short and intensive bursts of H_2O.

Quantitative data relating to each individual peak are summarized in Table 1. Note that all of the data are averaged, since only average FES flow rates during on-times were monitored. The predicted values took correct Orbiter attitude and altitude (259 km) into account. The model aided in the calculation of the column density for measured as well as predicted data. Calculation of the column density was necessary, since only return fluxes were measured. The model predicts column densities and return fluxes depending on velocity vector, as well as other variables. It therefore provides for relationships between column densities and return fluxes. These relationships are useful to deduce values for column densities when only return flux values are known.

Measured and predicted values for peaks (g) and (h) are correlated within a factor of 3 with measured data lower than those predicted. Measured values for peaks (b)-(d) appear to be about an order of magnitude lower than those predicted. Note that instantaneous values, e.g., for the column density, may be significantly higher than those averages, particularly during "bursts."

Measured and predicted values are correlated reasonably well, considering that 1) only average FES flow rates per peak are known, 2) the MS output therefore had to be averaged, 3) the measured output was not specifically related to the elevon angle, 4) the elevon angle was not monitored, and 5) predictions were available only for zero elevon angle. Predicted values appear to be close to the maximum obtainable. It appears that the maneuver at about 27.5 h MET changed elevon position and, with it, reflection characteristics.

Direct Flux Measurement

The STS-4 mission included a survey of the general contamination flowfield above the payload bay by direct measurement of flux from the various Orbiter sources with the IECM carried on the RMS. This survey lasted a total of 2 h 35 min, including unberthing and berthing of the IECM, while the MS operated at a high data rate (1 cycle/min). It incorporated 15 measurement points (each defined by MS location and direction). The Orbiter was in "top to sun attitude" to allow for maximum source flow rates. Five of these measurement points were dedicated to the measurement of flow from the FES, which is reflected off the left Orbiter wing in order to enable correlation with model data. Predictions were made for elevons in zero position. The crew confirmed, however, that the left elevons, particularly the inboard elevon, were turned

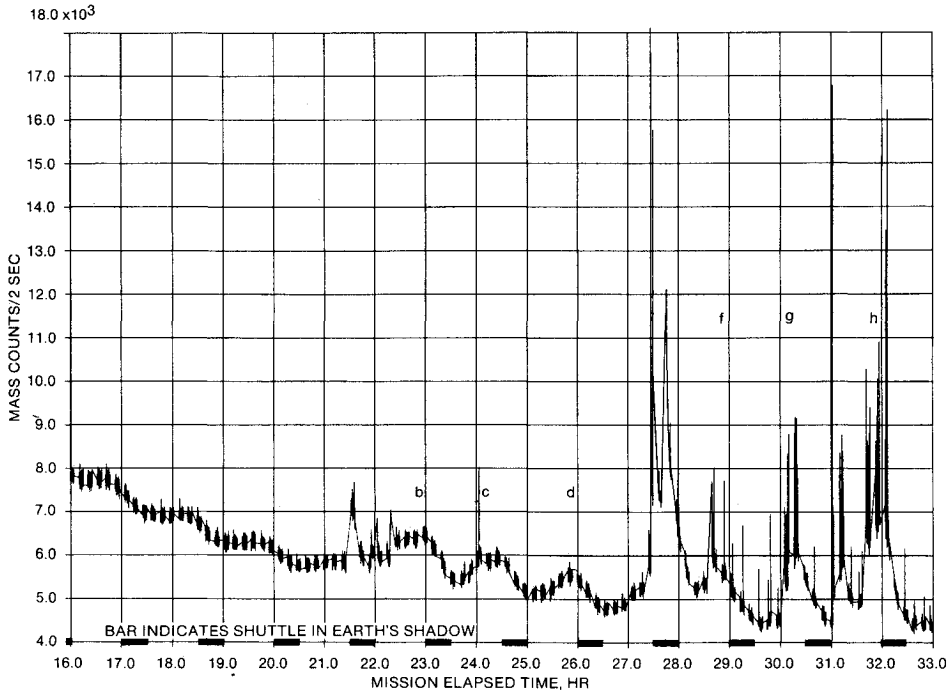

Fig. 9 Mass spectrometer output for amu 18 during the STS-2 mission.

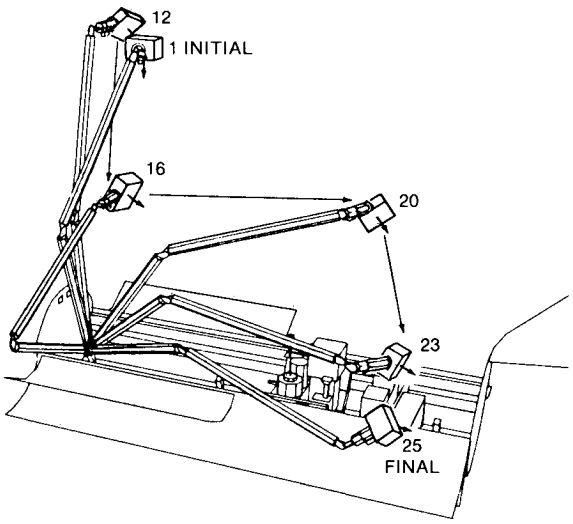

Fig. 10 The IECM and MS locations during the contamination survey of the STS-4 mission.

upward during the mission. As mentioned before, this case has not been modeled precisely. Nevertheless, the measurement results provide for interesting and useful information.

The FES was forced to operate for 3½ min (½ min flow buildup) at each of the measurement points 12, 16, 20, 23, and 25 (Fig. 10), while the thrusters were inhibited in order to record approximately three complete mass spectra. This time period was preceded by 4 min and followed by 2 min of thruster/FES inhibition. The 4-min time period was allocated to outgassing measurements, and the 2-min time period to allow for clearance of the FES vent pipes and H_2O vapor dissipation. The MS response is shown in Fig. 11. The measurement points marked by their identification numbers are clearly represented by peaks, with such discernible details as rising and decreasing flux. The larger unlabeled peaks, particularly those following the labeled peaks, are probably due to RCS operation for attitude restoration after the thruster inhibition periods. This conclusion, however, is not positively verified. The 0.5-min intervals of amu 18 output can be recognized. Larger measurement gaps affected two of the peaks (16 and 25), without significant loss of information, however. The Orbiter attitude in terms of angle between the $+Z$ axis and the velocity vector varied within the range of 8-176 deg throughout the survey. However, the MS output appears to be independent of this variation in attitude and increases somewhat when the Orbiter enters sunlight shortly after 46.4 h MET. The rates in Fig. 11 ranging from 600 (12) to over 5000 (25) counts/0.2 s were produced by an FES-emitted average flow of about 3 g/s.

It is, of course, desirable to compare measured results for different elevon positions and otherwise equal conditions; however, only the measured data in Fig. 11 are available. To assess the effect of elevon position on the local environment on the basis of these limited experimental data, a quantitative comparison was performed of the measured data and the model predicted values for zero elevon position. The results are shown in Table 2. Table 2 includes a column listing elevon-up data as a fraction of zero elevon prediction. The values in this column vary considerably. In order to understand this behavior, one must keep in mind that maximum reflection intensity exists on the elevon very near the vent and decreases rapidly with distance. This area of maximum reflection contributes significantly to the flux at points 12, 20, and 25. However, it does not contribute to point 16, because of flow blockage by the payload bay door. Therefore additional flow blockage by upturned elevons is less effective in the direction to point 16. The same area contributes only little to the prediction of point 23, since it appears to be located outside the MS collimator field of view of half-angle 10 deg.

In summary, turning the (inboard) elevons upward to a location above the FES vent resulted in a reduction of flow into directions not already blocked by either the OMS pods or the payload bay doors to within a few percent of the rate at zero elevon level.

It should be pointed out that ice particle formation has not been included in this FES data analysis, since it has not been detected in conjunction with FES operation either in flight or during functional tests on the ground.

Table 1 Return flux to the mass spectrometer (STS-2)

Peak	H_2O emission, g/s	Measured data: Sample rate, counts/2 s	Measured data: Return flux, $\times 10^9$ molecules/cm^2-s	Measured data: Column density, $\times 10^{12}$ molecules/cm^2	Predicted data: Return flux, $\times 10^9$ molecules/cm^2-s	Predicted data: Column density, $\times 10^{12}$ molecules/cm^2
b	2.9	255	2.0	1.4	36	26
c	1.4	163	1.3	0.9	17	13
d	1.23	116	0.9	0.65	15	11
f	1.24	325	2.5	1.8	15	11
g	1.3	557	4.3	3.1	16	12
h	1.3	789	6.1	4.4	16	12

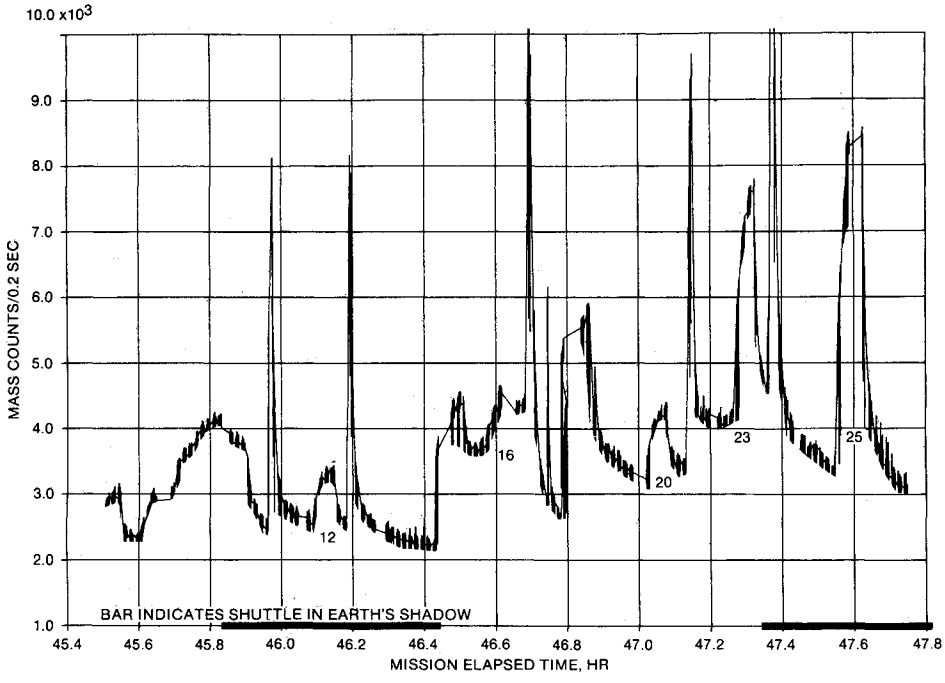

Fig. 11 Mass spectrometer output for amu 18 during the STS-4 mission.

Table 2 Direct flux to the mass spectrometer (STS-4)

Measurement number	Mass spectrometer output, counts/0.2 s: Predicted for zero elevon position ($\times 10^3$)	Mass spectrometer output, counts/0.2 s: Measured for elevon-up position ($\times 10^3$)	Ratio of measured to predicted elevon data, %
12	26	0.6	2.3
16	3.9	0.9	23
20	16	1.0	6.2
23	6.9	3.5	50
25	75	5.5	7.3

Conclusions

Analytical data provide the Shuttle user with an overall understanding of the character of the environment that is induced by the supplemental flash elevator system (FES). These data should be very helpful in deciding on actions required to provide optimal payload performance. These analytical data are supported by in-flight measurements within the relatively large range of measurement uncertainties of an order of magnitude. The level of H_2O contamination above the payload bay is significantly reduced when the elevons are turned upward. The goals stated in Refs. 1 and 2, which were defined for quiescent Orbiter mission periods, are generally not achievable during FES operations. For the limited number of measurements which may be affected by the FES effluent, the FES can be inhibited during critical times.

References

[1] "Space Shuttle Flight and Ground System Specification," JSC-07700, Vol. X, NASA Johnson Space Center, April, 1978.

[2] "Payload Contamination Control Requirements for Space Transportation System (STS) Induced Environment," STS Payload Contamination Requirements Definition Group Report, NASA Marshall Space Flight Center, July, 1975.

[3] Ehlers, H. K. F., Jacobs, S., Leger, L. J., and Miller, E., "Space Shuttle Contamination Measurements from Flights STS-1 through STS-4," *Journal of Spacecraft and Rockets*, Vol. 21, May-June 1984, pp. 301-308.

[4]Ehlers, H. K. F., "An Analysis of Return Flux from the Space Shuttle Orbiter RCS Engines," AIAA Paper 84-0551, Jan. 1984.

[5]"Shuttle Active Thermal Control System Development Testing," LTV Aerospace Corp., Vought Systems Division, Dallas, TX, Rept. T169-28, Vol. VI, Nov. 1973.

[6]Nason, J. R., Wierum, F. A., and Yanosy, J. L., "Challenges in the Development of the Orbiter Active Thermal Control Subsystem," NASA CP-2342, Part 1, 1985, pp. 450-464.

[7]Jarossy, F. J., Bareiss, L. E., Pizzicaroli, J. C., and Owen, N. L., "Shuttle/Payload Contamination Evaluation Program—Final Report," Martin Marietta Corp., Denver, CO, (Contract NAS9-15826), Rept. MCR-81-510, March 1981.

[8]Bhatnagar, P. L., Gross, E. P., and Krook, M., "A Model for Collision Processes in Gases—I. Small Amplitude Processes in Charged and Neutral One-Component Systems," *Physical Review*, Vol. 94, 1954, p. 511.

[9]Robertson, S. J., "Spacecraft Self-Contamination Due to Back-Scattering of Outgas Products," Lockheed Missiles and Space Company, Huntsville, AL, Rept. LMSC-HREC TR D496676, Jan. 1976.

[10]Miller, E. R. and Decher, R., "An Induced Environment Contamination Monitor for the Space Shuttle," NASA TM-78193, Aug. 1978, pp. 132-144.